HHS Public Access

Author manuscript

Free Radic Biol Med. Author manuscript; available in PMC 2016 May 01.

Published in final edited form as:

Free Radic Biol Med. 2015 May ; 82: 50–62. doi:10.1016/j.freeradbiomed.2015.01.012.

Hemoglobin induced lung vascular oxidation, inflammation, and remodeling contributes to the progression of hypoxic pulmonary hypertension and is attenuated in rats with repeat dose haptoglobin administration

David C. Irwin[#1,**], **Jin Hyen Baek**[2,*], **Kathryn Hassell**[3], **Rachelle Nuss**[3], **Paul Eigenberger**[1], **Christina Lisk**[1], **Zoe Loomis**[3], **Joanne Maltzahn**[1], **Kurt R Stenmark**[4], **Eva Nozik-Grayck**[4], and **Paul W. Buehler**[#2,1,*]

[1] Cardiovascular Pulmonary Research Group, Division of Cardiology, School of Medicine, University of Colorado Denver | Anschutz Medical Campus, Aurora, Colorado [2] Laboratory of Biochemistry and Vascular Biology, Office of Blood Research and Review, Center for Biologics Evaluation and Research, U.S. Food and Drug Administration, Bethesda, Maryland [3]Colorado Sickle Cell Treatment and Research Center, University of Colorado Denver | Anschutz Medical Campus, Aurora, Colorado [4] Cardiovascular Pulmonary Research Group, Pediatrics, School of Medicine, University of Colorado Denver | Anschutz Medical Campus, Aurora Colorado

[#] These authors contributed equally to this work.

Abstract

Objective—Haptoglobin (Hp) is an approved treatment in Japan with indications for trauma, burns and massive transfusion related hemolysis. Additional case reports suggest uses in other acute hemolytic events that lead to acute kidney injury. However, Hp's protective effects on the pulmonary vasculature have not been evaluated within the context of mitigating the consequences of chronic hemoglobin (Hb) exposure in the progression of pulmonary hypertension (PH) secondary to hemolytic diseases. This study was performed to assess the utility of chronic Hp therapy in a preclinical model of Hb and hypoxia mediated PH.

Approach and results—Rats were simultaneously exposed to chronic Hb-infusion (35 mg per day) and hypobaric hypoxia for five weeks in the presence or absence of Hp treatment (90 mg/kg twice a week). Hp inhibited the Hb plus hypoxia-mediated non-heme iron accumulation in lung and heart tissue, pulmonary vascular inflammation and resistance, and right ventricular

[**]Corresponding Author: David C. Irwin, Ph.D., Assistant Professor, 12700 East 19th Avenue, Research Building 2, Room 8121, Aurora, CO 80045, Phone: 303 724-3684, Fax: 303 724-3693, David.Irwin@UCDenver.edu.

[*]The findings and conclusions in this article have not been formally disseminated by the Food and Drug Administration and should not be construed to represent any Agency determination or policy.

Disclosures: The authors declare no conflicts

hypertrophy, which suggest a positive impact on impeding the progression of PH. In addition, Hp therapy was associated with a reduction in critical mediators of PH, including lung adventitial macrophage population and endothelial ICAM-1 expression.

Conclusions—By preventing Hb-mediated pathology, Hp infusions: (1) demonstrate a critical role for Hb in vascular remodeling associated with hypoxia; and (2) suggest a novel therapy for chronic hemolysis associated PH.

Keywords

Hemoglobin; heme; iron; lipid peroxidatio; hemolysis; sickle cell disease; thalassemia

INTRODUCTION

Pulmonary hypertension (PH) affects a disproportionately large percentage of patients who concurrently suffer from hemolytic anemia syndromes[1-3]. Recently, the World Health Organization (WHO) has re-categorized cases of PH that are concomitant with hemolytic syndromes from group 1 to group 5, which are described as “PH with unclear multifactorial mechanisms”[4]. PH is generally characterized by pulmonary vascular remodeling affecting the pre-capillary vessels and is associated with thickening of the intimal, medial, and adventitial layers of the vascular wall[5-7]. The pathology of PH in individuals suffering from hemolytic syndromes is likely complex and impacted by a number of factors. In SCD, however, these conditions are characterized by exposure of the pulmonary vasculature to chronic low concentrations of extracellular hemoglobin in the setting of a pro-inflammatory and tissue-hypoxic background due to vaso-occlusion and ischemic reperfusion events[1, 8]. Our group recently developed and characterized an animal model to investigate the pulmonary vascular effects associated with chronic exposure to extracellular Hb in the presence or absence of tissue hypoxia[9]. Our model shares phenotypic similarities with hemolytic diseases by condensing a life time of intermittent Hb and Hx exposure into a time frame that approximates hemolysis and tissue hypoxia derived from episodes that reduce or inhibit oxygen supply to the pulmonary microenvironment[1, 8, 9].

The hemolysis of red blood cells and accumulation of extracellular Hb elicit numerous biochemical, biological, and physiological changes that impact the development and progression of PH. These include interactions between Hb and nitric oxide (NO), superoxide, or hydrogen peroxide. Hb is a known NO scavenger, which causes depleted NO bioavailability resulting in persistent vasoconstriction. Furthermore, Hb interacts with superoxide and hydrogen peroxide to increase reactive oxygen species (ROS) formation and lipid peroxidation[10], which in turn potentiates, inflammation, vascular tissue injury and endothelial damage. In addition, the components of Hb, globin or heme are postulated to interact with specific cellular immune receptors, such as toll-like receptor 4 (TLR4)[11-13], which can perpetuate chronic pulmonary vascular inflammation[14].

Although extracellular Hb accelerates the development and progression of pulmonary vascular disease, a specific and effective therapy is not yet available. The recognition that Hb may be directly involved in the pulmonary pathology associated with hemolytic diseases has piqued interest in developing Hb/heme scavenging proteins and peptides as potential

therapies of pulmonary vascular disease associated with hemolytic anemia syndromes. Haptoglobin (Hp), the endogenous Hb scavenger in human plasma consists of three primary phenotypes (Hp 1-1, Hp 2-1 and Hp 2-2) that circulate within a plasma concentration range of 0.3 – 1.9 mg/mL [15, 16]. The three Hp isoforms all contain the same Hb binding β-globin (Hp^{β}), but differ in their α-globin ($Hp^{\alpha 1}$ or $Hp^{\alpha 2}$) composition[17, 18]. It is the α-globin chain composition that defines dimeric (Hp 1-1) or multimeric/polymeric (Hp 2-1, Hp 2-2) forms of the protein. Several studies have shown that infusion of dimeric and multimeric Hp prevents Hb renal excretion and subsequent kidney injury following acute hemolysis[19, 20].

Utilizing our recently developed and characterized animal model of chronic Hb infusion (Hb concentrations of 3–15 μM and relevant to hemolytic disease syndromes[21]) that phenocopies pulmonary vascular disease associated with hemolytic syndromes [9]; Herein we test the hypothesis that twice weekly Hp dosing could provide an effective means of neutralizing oxidation, inflammation, pulmonary vascular remodeling and right ventricular changes in the progression of hypoxic PH.

METHODS

Animals

Male Sprague-Dawley rats were obtained from a commercial vendor (Charles River, Wilmington, MA). All experimental protocols were reviewed and approved by the Institutional Animal Care and Use Committee at University of Colorado Denver | Anschutz Medical Campus. All animals survived the surgical procedure and subcutaneous implantation of the iPRECIO® pumps. None of the rats exhibited any signs or symptoms indicative of systemic infection. Following surgery, wounds healed within 10 days.

Hypoxia model

Chronic hypoxia was induced in rats by continuous exposure to a simulated high altitude (5,500 m; 18,000 ft; Pb= 380 mmHg;) in a specially designed rodent hypobaric chamber facility[9, 22]. This model previously demonstrated that chronic hypoxia (10% O_2) increased pulmonary arterial pressure, pulmonary vascular remodeling and right ventricular hypertrophy[9, 22].

To further study the effects of extracellular Hb and attenuation by Hp therapy, animals were randomly assigned to one of five groups: **(1)** Normoxic control (NX); **(2)** Hypoxic control (HX); **(3)** Hp+HX twice weekly (90 mg, 1.5 ml I.V. injection, Hp) **(4)** Hb infusion + HX (35 mg/day Hb); supplemented with injections of Hp twice weekly (90 mg/kg, 1.5 ml I.V. injection, Hp); **(5)** HX + Hb infusion (35 mg/day Hb). The study was replicated twice, with a minimum of six animals in each replicate and a minimum of fourteen animals per group were evaluated. All animals were euthanized after final hemodynamic monitoring at five weeks post-study initiation.

Hemoglobin and haptoglobin

Purified human endotoxin free Hb (LPS < 0.5 endotoxin units, EU) was prepared from outdated blood as previously described[23]. Further, catalase and superoxide dismustase was

removed using an ÄKTA FPLC system and an XK 16/70 column containing Superdex 200 medium or an XK 50/100 column containing Sephacryl 200 medium (GE Healthcare Bio-Sciences, Piscataway, NJ, USA). The sample volume was <1% of the column bed volume, sample concentrations for each injection were 50 mg/ml, and flow rates were set to 1.0 ml/min. Samples were filtered through 0.45-μm pore size syringe filters before loading onto the column (EMD Millipore, Billerica, MA, USA). All Hb purification steps were performed at 4 °C using 50 mM potassium phosphate buffer, pH 7.0 at 22 °C and elution of protein was monitored at a wavelength (λ) = 280 nm. After collection, Hb solutions were concentrated to 100 mg/ml using 30 kD cut-off Centricon centrifugal filter devices (Millipore, Billerica, MA, USA). The starting composition of Hb was 96.5 ± 1.3% ferrous and 3.50 ± 0.23% ferric Hb. The following molar extinction coefficients and absorption wavelengths were used to calculate concentrations, 15.2 mM^{-1} cm^{-1} at 576 nm (ferrous, oxyHb) and 4.4 mM^{-1} cm^{-1} at 630 nm (ferric, metHb) in 50 mM, phosphate buffer, pH 7.2, ambient temperature in a 1 cm path length cuvette[24]. Hp was supplied by Bio Products Laboratory Ltd. at a concentration of 60 mg/ml. The preparation contained primarily Hp 1-1 (dimeric form), however measurable polymeric forms, including Hp 2-2 and Hp 2-1 (15-16.5 min elution time) were observed by size exclusion chromatography following the addition of Hb (see red trace standard, **Figure 1B**). To prepare Hb-Hp complexes for in vitro assays, $HbFe^{2+}$ was added to Hp in a 2:1 ratio (1.2 ml (120 mg) Hb to 1 ml (60 mg) Hp. Free Hb was removed from the Hb-Hp complex by injecting 5 ml of mixture onto a semi-preparative BioSep-SEC-S3000 (600 × 21.2 mm) column (Phenomenex, Torrance, CA) with 50 mM Potassium Phosphate, pH 7.4 as the mobile phase monitored at absorbance wavelengths (λ) = 280 nm and (λ) = 405 nm. Collections of Hb-Hp at 12-17 minute elution times were obtained, pooled and concentrated to heme concentration of 50 μM. MetHb and metHb-Hp complexes were prepared by adding a 10-fold molar excess of potassium ferricyanide from a 20 mM stock solution. Samples were mixed for 5 min at 4°C and conversion from the Fe^{2+} to the Fe^{3+} state was followed using uv-visible spectrophotometry over a absorbance wavelength range from (λ) = 450 −750 nm. $HbFe^{3+}$ was then added to a gravity flow column filled with 30 ml of Sephadex G-25 medium (Biorad Laboratories, Philidephia, Pa) in 50 mM PBS, pH 7.0. Samples were collected and washed 5 times (10 ml each) with 0.9% NaCl to remove any residual ferricyanide. To ensure the removal of catalase from our initial separation, an activity assay for the enzyme in our Hb preparations was run according to published methodology [25].

Micro infusion pump placement

Programmable micro infusion pumps (iPRECIO®, Tokyo, Japan) were placed subcutaneously according to the manufacturer's protocol and as previously described[9]. iPRECIO® pumps were programmed to deliver Hb at a dose (35 mg/day or 250 μg • $μL^{-1}$) or saline at an infusion rate 6 μL per hour, and were refilled with fresh aliquots of Hb every 3 days for five weeks. At an infusion rate of 35 mg per day, we have previously shown that total plasma heme concentrations were in a close range of values that approximate a mild to moderate chronic hemolytic state [9, 21]. All animals tolerated the surgical procedure for pump implantation well, without any fatalities, and wounds were healed within ten days after the procedure in all animals. Residual pump Hb was analyzed prior to refilling and

demonstrated the following mean residual compositions: 84.3 ± 6.0% ferrous, 11.2 ± 7.3% ferric, and 6.6 ± 6.2% hemichrome.

Plasma Hb analyses

In order to examine the steady state pharmacokinetics and Hb binding following Hp infusions, blood samples were taken via the tail vein of normoxic animals infused with Hb in the presence or absence of Hp therapy at days 1, 4, 8, 16, 30, and 34. Plasma concentrations of Hb were determined using a photodiode array spectrophotometer (Model 8453 Hewlet Packard, Palo Alto, CA). Plasma from baseline samples of each animal was used to correct for background interference and turbidity. Ferrous ($HbFe^{2+}$) Hb (oxy/deoxy), ferric Hb ($HbFe^{3+}$), and hemichrome were determined using multi-component analysis based on the extinction coefficients for each species, and total heme was calculated by adding these values and converting heme concentration to total Hb (Winterbourn CC (1985) In CRC Handbook of Methods of Oxygen Radical Research; Greenwald, RA Ed.; CRC Press: Boca Raton FL; pp 137-141). Plasma samples were separated on a analytical BioSep-SEC-S3000 (600 × 7.5 mm) column (Phenomenex, Torrance, CA) with 50 mM Potassium Phosphate, pH 7.4 as the mobile phase monitored at λ=280 nm and λ=405 nm. Hb bound to Hp and unbound in plasma was determined by dividing the Hb peak area and the Hb-Hp peak areas by additive areas under the Hb-Hp chromatographic peak (12-17 minute elution) and the Hb chromatographic peak (21 minute elution) at λ=405 nm.

Hemodynamics

Pulmonary and arterial blood pressures were determined at the end of 5 weeks; indwelling, fluid-filled catheters were placed in the jugular vein and carotid artery of rats and the signal was captured with the Biopac system. Cardiac output was measured by dye dilution method from infusion of cardiogreen (Sigma Aldrich, St. Louis, MO) utilizing specially designed densitometer and software (Deterministic Systems Design, Longmont, CO). Total pulmonary and peripheral vascular resistance index was calculated as a mean pulmonary or systemic arterial pressures (PAP, MAP respectively) / cardiac output.

Blood and organ collection

After hemodynamic measurements, animals were exsanguinated via the carotid catheter; blood was placed in chilled heparinized vacuum tubes and centrifuged. The plasma was removed, frozen in liquid nitrogen and stored at −80°C until analysis. The aorta was severed and the lungs were perfused with PBS (5 mL) via the right ventricle to remove blood. The left lungs were tied off at the left main bronchus, removed and snap frozen. The right lung was fixed with 10% buffered formalin (~3 mL) by airway inflation under constant pressure at 25 cm H_2O pressure. After which, the heart and lungs were removed en bloc. The hearts were removed and the atria were dissected from ventricles. The right ventricle (RV) and left ventricle + septum (LV+S) were weighed for assessment of right ventricular hypertrophy (RV/LV+S). After 18 hours the lungs were removed from 10% formalin and placed in 70% ethanol and prepared by standard methods for morphometric and immunostaining analyses.

Plasma IL-6 quantification

Whole blood from treated and untreated rats was collected in Lithium Heparin blood tubes (VWR, Pennsylvania, USA) at time of euthanasia/tissue harvesting and immediately spun down at 5,000 g for 10 minutes at room temperature. Plasma samples were separated into aliquots and immediately frozen in liquid nitrogen to be stored at −80° C. A V-Plex Pro-inflammatory Panel 1 (rat) Kit was purchased directly from Mesoscale Discovery (Maryland, USA). Plasma samples were diluted 4-fold in Diluent 42 (provided) and run in triplicate according to manufacturer protocols. The assay was imaged on a Mesoscale SECTOR Imager 2400.

Morphology and immunohistochemistry of lung tissue

Five-micron sections of formalin–fixed, paraffin-embedded lung tissue were stained with hematoxylin and eosin by standard procedures at the University of Colorado Histology Core to assess the accumulation of perivascular cells as well as vessel wall thickness. A separate set of lung sections were stained for smooth muscle actin and developed with 3,3'-Diaminobenzidine (DAB) for quantification of small arterial muscularization.

Three fields were photographed on each slide utilizing a Nikon microscope. Positively stained smooth muscle vessels were counted and described as either fully or partially muscularized. Any area that fell outside the lung boundary was subtracted from total area, and the number of either, fully or partially muscularized vessels, was normalized to area. Distal pulmonary vessels (outside diameter 10-50 μm) were assessed for degree of circumferential α-smooth actin-positive staining indicative of muscularization utilizing a Nikon microscope programmed to photograph an area of 35,512 μm^2 (218 μm by 163 μm); Proximal vessels (outside diameter 50-250 μm) were analyzed for medial wall thickness at four points around the vessel circumference and for lumen diameter along two axes. Wall thickness is expressed as the ratio of medial wall thickness to lumen radius.

Histological analysis for non-heme iron deposition in lung and cardiac tissue was detected using Perls method with diaminobenzidine (DAB) intensification as previously described [26]. For image analysis of iron staining cells per field, a total of 20 images at 20x magnification were obtained from the stained tissue sections of all animals. Within each of the 20 images the total number of cells were counted and divided by 20.

Immunohistochemistry analysis for α-smooth muscle actin, factor-XIII, 4-hydroxynonenal, heme oxygenase 1 (HO-1), CD163, inter-cellular adhesion molecule 1 (ICAM-1) was performed per the manufacturer's instructions. Antigen retrieval was performed on serial lung sections and then incubated with antibodies against HO-1 (4 μg/mL, abcam, ab13243, Cambridge, MA), CD163 (1:100 Trillium diagnostics, CD163-48U, Brewer, MA) or ICAM-1 (1:300, Pierce, MA1-80472, Rockford, IL). Lung sections were incubated with a fluorescent secondary antibody (either Alexa Fluor 488 (1:300 or 1:800) or Alexa Fluor 555 (5 μL/mL) Invitrogen, Carlsbad, CA). Pulmonary vessels (outside diameter 20-300 μm) were assessed for the presence of, HO-1, CD163 or ICAM-1 protein expression on a Nikon Eclipse T*i*-E inverted epi-fluorescent microscope (Nikon Instruments, Tokyo Japan).

HO-1 (mouse monoclonal anti-HO1, abcam ab13248), ICAM-1 (mouse monoclonal anti-ICAM, abcam ab2213) protein concentrations were determined from total lung protein content by standard western blot technique. Briefly, analysis was performed using 50 μg of sample protein run under denaturing and reducing conditions on NuPAGE bis-tris 4-12% gels with an Xcell II blot system (Invitrogen, Carlsbad, CA). With the exception of probing for ICAM-1 all protein for immuno blots were run under denaturing and reducing conditions on NuPAGE bis-tris 4-12% gels with an Xcell II blot system (Invitrogen, Carlsbad, CA); the probing for ICAM-1, protein was utilized under denaturing and non-reducing conditions. HO-1 and ICAM-1 bands were normalized to beta actin. Statistical analysis was determined from fold difference of NX CTRL on the same gel. Gels were imaged on an Alpha Innotech gel documentation system (Protein Simple, Santa Clara, CA) and densitometric analyses were performed using ImageJ software (version 1.44o, National Institutes of Health, USA).

PCR analysis

Total lung RNA was isolated using Qiagen RNeasy Plus Mini Kit with gDNA filter column (Qiagen, California, USA). RNA was quantified spectrophotometrically (NanoDrop-1000), and equal amounts (1 μg) were loaded with Quanta cDNA Supermix (Quanta, Maryland, USA) for cDNA synthesis. cDNA was diluted five-fold in TE buffer for downstream reactions. Primers for rat-CD163 (Qiagen QuantiTect QT00449113), rat-ITGAM1 (Qiagen QuantiTect QT00495565), and rat-ACTB (Qiagen QuantiTect QT00193473) were used in reactions with 250 ng cDNA and Quanta PerfectCTa SYBR Green Master Mix, ROX. 96-well PCR plates were run on Applied Biosystems AB7300 (ThermoFisher, Maryland, USA), with reaction cycling of initial denaturing (95 C, 2 min), followed by 40 cycles of denaturing (95 C, 15s), annealing (55 C, 30s) and extension (72 C, 30s). A melting curve was run to confirm specificity of PCR products. Experimental and reference genes were run on separate plates on the same day and relative quantification determined by the delta-CT method.

Cell culture experiments

Rat Pulmonary Endothelial Cells (RPAEC) were kindly provided by Dr.Troy Stevens at University of Southern Alabama and cultured in Dulbeco's Modified Growth Medium (DMEM) supplemented with 10% fetal bovine serum, 50 units/mL Penicilin, 50 ug/mL Streptomycin, 1 μg/mL Fungizone Anitmycotc (Life Technologies, New York). Cells were cultured under standard conditions (21% O_2, 5% CO_2, balance N_2), passaged 1:4, and used between passages 5-10 for all experiments. Cells were checked daily for morphological changes in a cobblestone appearance that would suggest an alteration in phenotype. Prior to experimental conditions, cells were quiesed in fresh DMEM containing 0.2% FBS for 24 hours.

Click-iT Lipid Peroxidation Assay

RPAEC were seeded 10,000 cells per cm^2 on 4-well, 1.0 mm, glass chamber slides (Electron Microscopy Sciences, Pennsylvania) and grown to confluency. Cells were treated with DMEM (Sigma Aldrich, Missouri) containing 0.2% FBS, 50 μM Click-iT linoeamide alkye (Life Technologies, New York) and exposed to hypoxia in the presence or absence of 6.25 μM superoxide dismustase/catalase depleted human $HbFe^{2+}$, $HbFe^{3+}$ and pre-formed Hb-Hp complex with Hp bound to human $HbFe^{2+}$ or $HbFe^{3+}$. Hypoxia was induced in an air-

tight, humidified, cell culture chambered flushed with 1% oxygen. Cells were exposed to Hb and Hx for 6 hours then immediately washed with PBS and fixed in 3.7% formalin for 10 minutes at room temperature (all subsequent steps were performed at room temperature). Cells were permeabilized with 0.5% Triton x-100 for 10 minutes and blocked with 1% BSA for 30 minutes. After three washes in PBS, the cells were stained with the Click-iT reaction cocktail for 30 minutes in the dark. After three washes in PBS, a nuclear stain was performed using Hoechst 33342 (2 μg/mL). Imaging was conducted on Nikon Eclipse T*i*-E inverted epifluorescent microscope (Nikon Instruments, Tokyo Japan). As a positive control for the pro-oxidative environment created under hypoxia, the same groups were evaluated under normoxia with the addition of 10 mU of glucose oxidase (GOX, type X-S derived from *Aspergillus niger*, Sigma Aldrich, Saint Louis, MO). The % fluorescence was quantified using the Fiji distribution of ImageJ (Marlyand, USA). Briefly, a threshold analysis was used to select stain positive pixels on 60x magnification images. Nuclei were excluded by adjusting the Hue to exclude blue wavelengths. Stain positive pixel area was measured and compared to total area of image area. Process was repeated using up to seven separate images per group.

Statistical Analysis

For all groups, mean ± S.E.M is reported. Statistical comparisons for data measurements were completed with multi-factorial analysis of variance (ANOVA) and included determination for the main effects from Hb exposure, hypoxia, and Hb + Hp treatment. Main effects were determined by combining all Hb or saline infused groups, normoxia or hypoxia exposed groups, and Hp treated or untreated groups. Post-hoc analyses were completed with unpaired, two-sided Student's *t*-test with a Bonferroni adjustment unless otherwise noted. Statistical analyses were performed using JMP (Version 5) statistical software package (SAS; Cary, North Carolina) with statistical significance set at $p \leq 0.05$.

RESULTS

Hb exposure and intra-vascular Hb-Hp complex formation

Continuous infusion of 1.46 mg/hr of Hb led to a steady state plasma concentration of 13.6 ± 2.2 μM heme (219 mg/L Hb) over five weeks. The percentages of unbound and Hp-bound Hb were determined by SEC-HPLC analysis in plasma collected from animals after Hp administration. Over the initial week of Hb exposure, Hp administrations lead to the binding of 31.7 ± 6.0% and 51.7 ± 4.4% of circulating Hb after the first and second doses, respectively. Following the third dose and until study termination, Hb in the plasma was 100% bound to Hp (**Figure 1A**). Chromatography of plasma from representative Hb exposed and Hp administered animals demonstrated a free Hb peak at an elution time of 21 minutes. This was confirmed by the chromatographic profile of Hb standard solution shown as a dotted red trace. An elution time shift to a broad band of peaks eluting over 13-17.5 minutes was observed as extracellular plasma Hb became bound to Hp. This was consistent with the elution time profile of the Hb-Hp standard shown as a solid red trace consisting of three primary peaks at 15.5, 16.5, and 17.5 minutes (**Figure 1B**). These data confirm that the Hp dose used in this study was effective at scavenging extracellular Hb within the plasma compartment.

Hp prevents pulmonary vascular iron deposition and accumulation of CD163^{+}/ HO-1^{+} cells

Localization of non-heme iron was observed in the medium and small blood vessels of Hb exposed rats. Lung sections from NX animals did not reveal any non-heme iron deposition and only sporadic visualization was observed in HX and Hp+HX animals (**Figure 2A-C**). Exposure to Hb + HX showed diffuse regions of lung iron accumulation after five weeks that was prevented by Hp administration (**Figure 2D**). Non-heme iron staining was primarily observed in the intima, media, and adventitia of small and medium sized pulmonary blood vessels, as well as the vasa vasorum of larger blood vessels. Under high magnification (100x), cells containing iron were observed to accumulate within the perivascular regions of medium sized pulmonary vessels (**Figure 2D, high magnification, 100x**). Iron accumulation was prevented by Hp administration during continuous exposure to Hb **(Figure 2E)**. Visual counting of iron positive cells per image field for each group showed a significant increase in Hb + HX animals compared to all other groups **(Figure 2G)**. These data suggest that Hp may prevent extravascular translocation of Hb and iron deposition within the pulmonary vasculature or limit the accumulation of inflammatory cells in the adventicia. Our previous work supports the concept that Hb and not non-transferrin bound iron is the source of deposition in the vasculature, as chelation therapy did not prevent tissue iron accumulation in a guinea pig model of extra-cellular Hb exposure [26].

Heme oxygenase-1 (HO-1) is a critical enzyme in the process of Hb detoxification and a relevant marker of localized sites of Hb exposure. To confirm the identity of HO-1-expressing cells, lung sections were co-stained for HO-1 and CD163, a specific marker of monocytes/macrophages Hb scavenger cells and commonly associated with a macrophage “activation” phenotype. In NX animals, CD163^{+} perivascular cells co-expressing low HO-1 were minimally detectable near small to medium-sized blood vessels (**Figure 3C**). Animals exposed to HX and Hp + HX demonstrate moderate accumulation of CD163^{+}/HO-1^{+} in perivascular cells (**Figure 3C**). In contrast, Hb + HX exposed animals showed a marked increase of perivascular accumulation of CD163^{+}/HO-1^{+} cells around small to medium-sized pulmonary blood vessels (**Figure 3C**). CD163^{+}/HO-1^{+} infiltrates were also identified within the lumen of many blood vessels. Hp administration decreased the extravascular accumulation of CD163^{+}/HO-1^{+} cells, particularly within the adventitial regions around blood vessels (**Figure 3C**).

Hb-mediated pulmonary vascular lipid peroxidation is reduced by Hp

Tissue accumulation of non-heme iron can lead to an increase in reactive oxygen species and lipid peroxidation products. Hp administration decreased tissue non-heme iron accumulation, thus we hypothesized it would also attenuate Hb mediated lipid peroxidation in lung vasculature of Hx and Hb exposed rats. We visually contrasted lung tissue stained for 4-hydroxynonenal (4-HNE), a marker for lipid peroxidation. Lung sections from the Hb + HX group showed lipid peroxidation throughout the vessel wall and in cells within the adventitia **(Figure 4).** While lung sections from the HX, Hp + HX and Hb-Hp + HX cohorts show evidence of lipid peroxidation compared to NX control animals, the intensity and abundance of positive stained cells is less than that of Hb + HX animals **(Figure 4).**

Hp directly inhibits Hb-mediated lipid peroxidation in pulmonary endothelial cells *in vitro*

To verify our in vivo data that show chronic Hb infusion causes vascular lipid peroxidation that is attenuated by Hp administration, we treated HX exposed rat pulmonary arterial endothelial cells with $HbFe^{2+}$ and $HbFe^{3+}$ in the presence or absence of Hp. Fluorescent microscopy show lipid peroxidation occurs by 6 hours in cells exposed to HX, which increases in the presence of either $HbFe^{2+}$ or $HbFe^{3+}$ **(Figure 5).** These data support our in vivo observations that Hp inhibits Hb-mediated lipid peroxidation. Additionally, the protective effect of Hp on Hb induced lipid peroxidation was observed in under NX conditions +/− GOX supplementation (data not shown).

Hb-induced vascular inflammation is reduced by Hp

Oxidative stress is linked with, and in some cases precedes, inflammation. We previously reported that chronic Hb exposure increased both the pro-inflammatory transmembrane receptor, ICAM-1 in and around the pulmonary vasculature, and plasma IL-6 concentrations [9]. Consistent with our previously reported results, either Western blot or plasma analysis from the present study demonstrates that Hb + HX exposed rats have increased expression of ICAM-1 and plasma IL-6 compared to NX, HX, and Hp + HX animals; furthermore, Hp treatment attenuated the expression of ICAM-1 (**Figure 6A**) and plasma IL-6 compared to Hb + HX exposed animals **(Figure 6B).** Immunofluorescence staining demonstrated increased ICAM-1 co-localization with Factor VIII, identifying its expression on vascular endothelial cells in lung sections from animals exposed to Hb + HX. Hp treatment reduced both the number of cells expressing ICAM-1 as well as intensity of ICAM-1 immunostaining on vascular endothelial cells (**Figure 6C**). $ICAM\text{-}1^+$ cells co-expressing CD163 were also present in the perivascular space (**Figure 6D**). Hp treatment decreased the accumulation of ICAM-1 expressing cells surrounding pulmonary blood vessels following Hb + HX exposure. Overall the accumulation of extravascular cells expressing $CD163^+/ICAM1^+$ was similar in lung sections from NX, HX, and Hp + HX exposed animals, however a greater accumulation of $CD163^+/ICAM1^+$ was observed in Hb + HX animal tissue sections (**Figure 6D**).

Hp decreases pulmonary vascular remodeling following Hb exposure

A hallmark of HX-induced PH is vascular remodeling characterized by medial wall hypertrophy and increased muscularization of small vessels associated with perivascular inflammation[5-7, 22]. These morphological changes were consistent with iron deposition, macrophage infiltration and ICAM-1 expression, supporting the outside to inside vascular remodeling paradigm proposed by Stenmark et al.[27]. Morphological and histological analyses were performed to evaluate the pulmonary vascular changes induced by concomitant Hb exposure plus HX on the progression of PH in the presence and absence of Hp. Chronic low level Hb + HX exposure lead to a greater visualization in the number of blood vessels staining positive for smooth muscle actin, conversely Hp treatment decreased the number of actin positive vessels in lung sections (**Figure 7A).** Hb + HX exposure increased the medial wall thickness in proximal arteries (outside diameter 50-250 microns), accumulation of adventitial cells, and the extent of muscularization in distal vessels (<10-50 microns in outside diameter) (**Figure 7A-C**). Hp treatment attenuated the effects of Hb plus

HX on the extent of small artery muscularization, reduced medial hypertrophy by normalizing lumen diameter of medium and large arteries and reduced the accumulation of adventitial neutrophils / macrophages (**Figure 7A-C**).

Hp improves pulmonary arterial blood pressure, myocardial function, and right ventricular iron deposition

As indicators for the progression of PH, we evaluated cardiac output, pulmonary hemodynamics, and the Fulton index (RV/LV+S) for each animal.

Hemodynamic Analysis—The combination of Hb + HX exposure resulted in a 30% reduction in cardiac output compared to rats exposed to hypoxia alone (**Figure 8A**). Hb exposure caused a trend toward increased PA pressures compared to hypoxia alone (**Figure 8B**), but a more severe progression of PH in the Hb exposed animals was reflected by a significantly increased (60%) pulmonary vascular resistance (**Figure 8C**). Consistent with the hemodynamic changes, the Fulton index (RV/LV+S) was significantly greater (25%) in Hb + HX groups compared to HX alone cohorts (**Figure 8D**). Taken together, the overall hemodynamic profile of the Hb + HX cohorts is consistent with more pronounced PH, when compared to all other groups. Hp treatment attenuated the Hb-mediated drop in cardiac outputs and normalized pulmonary vascular resistance, pulse pressure, and the Fulton index to hypoxia alone.

Myocardial iron deposition—At five weeks, the changes in right ventricular (RV) hypertrophy tracked with PA pressures and localization of RV non-heme iron deposition was observed in Hb exposed rats. RV heart tissue sections from NX animals did not show non-heme iron deposition. Similar to lung tissue (Figure 3), only sporadic accumulation of iron was observed in the HX and Hp + HX cohorts (**Figure 9**). We observed diffuse regions of RV myocardial iron deposition that were evident in cardiomyocytes and within the adventitia of the RV coronary arteries in the cohort exposed to Hb + HX (**Figure 9**). Collectively, Fulton index and RV iron accumulation data suggests iron deposition in the RV is associated with an inappropriate response to elevated pulmonary arterial pressures.

DISCUSSION

Until recently, hemolysis-associated PH was postulated to result primarily from NO depletion caused by extracellular Hb [1-3]. NO bioavailability remains an important component of hypoxia induced PH. This has been demonstrated in studies showing eNOS deficient mice exposed to hypoxia induce a near doubling of hypoxic pulmonary vasoconstriction compared to wildtype mice [28]. This suggests that NO scavenging in the lung micro-environement contributes to pulmonary vascular remodeling during hypoxia. However, it is now being recognized that the contribution of Hb to PH progression is more complex than NO scavenging alone. Thus, when discussing therapies that target Hb mediated pulmonary vascular pathology one should consider the multi-factorial toxicity of Hb, globin chains, heme, iron, and the corresponding biochemical and physiological effects[10]. As such, it has been proposed that the Hb and heme scavenger proteins, alone or in

combination, may be a therapeutic option to protect the vasculature against extracellular Hb [10, 11, 19, 29, 30].

To date, all preclinical studies evaluating Hp as a potential therapeutic have evaluated hemolysis in the acute setting. Here, we demonstrate in vivo proof of concept following multiple administrations of Hp in a preclinical model of chronic extracellular Hb-mediated progression of PH. In our model, twice weekly Hp treatment of 90 mg/kg reduced the severity of PH in rats chronically exposed to five weeks of extracellular Hb and concomitant HX. This effect was associated with suppression of lung and heart iron deposition, pulmonary vascular inflammation, systemic IL-6, medial thickening of pulmonary arteries, small arterial muscularization, and right ventricular hypertrophy. Based on the current studies data that demonstrates a reduction in both in vitro and in vivo lipid peroxidation in rat vascular cells and tissue, we speculate that the efficacy of Hp in preventing the progression of PH was principally due to its ability to bind and prevent extracellular Hb extravasation and subsequent extravascular accumulation of non-heme iron in the lungs and heart. These data are consistent with our previous results of chronic Hb infusion, and support the concept that Hb contributes to pulmonary vascular disease in part by pro-oxidative and pro-inflammatory mechanisms.

Tissue Hb accumulation results in macrophage infiltration, iron loading, localized generation of lipid peroxidation, pro-inflammatory cytokines and up-regulated tissue markers of inflammatory response [31]. Our data suggests Hb extravasates into the perivascular space, particularly in the vaso vasorum, and mediates tissue lipid peroxidation, which is followed by the migration of infiltrating cells loaded with iron and increased ICAM-1. Recent findings in the field of PH suggest a wide spectrum of macrophage phenotypes that are mechanistically linked to the pulmonary vascular remodeling process in both animal models as well as human PH[7, 22, 27, 32, 33]. Further, it has been postulated that leukocytes/macrophages recruited to the adventitia secrete inflammatory and growth factors that perpetuate pulmonary vascular remodeling in an “outside-to-inside” fashion [7, 27, 32, 33]. In our study, the same regions of iron deposition demonstrate an accumulation of macrophages co-expressing CD163 and HO-1, which is indicative of the Hb clearance macrophage (HA-Mac). The HA-Mac phenotype expresses high levels of proteins associated with the Hb detoxification pathway ($CD163^+$/$HO\text{-}1^+$), mannose receptor, and suppressed expression of HLA class 2 [34]. Paradoxically, in many of the same locations as the HA-Mac, we also observed an abundance of adventitial cells consisting of high CD163 and ICAM-1 co-expressing cells, with decreased HO-1. These data indicate a significant contribution by a non HA-Mac phenotype, in association with an increased number of adventitial cells, indicating a pro-inflammatory macrophage phenotype. This lends additional support to the concept that macrophages play a key role in an “outside-to–inside” fashion in the pulmonary vascular remodeling process. However, future characterization of our Hb-mediated PH model will need to clarify: 1) where these activated macrophages fall within in the macrophage spectrum; 2) what their exact contribution is to pulmonary vascular remodeling; and 3) their relationship, if any, to the HA-mac phenotype. These are all questions that require more detailed studies.

The Fulton index of right ventricular hypertrophy tracked with pulmonary pressures and resistance at the termination of the study and was accompanied by greater iron deposition in heart tissue. These data suggest that extracellular Hb not only contributed to pulmonary vascular remodeling, but may play a role in the progression towards right ventricular failure independent of PA pressures. It has previously been shown that myocardial iron causes myocyte apoptosis, inflammation, and cardiac dysfunction in transfusion dependent β-thalassemia patients[35]. We suspect that Hb mediated mechanisms of iron deposition and subsequent toxicity occurs in the right ventricle of our model. This could result in an Hb-induced dysregulation of normal compensatory right ventricular hypertrophy response that leads to right ventricular failure. Thus, the Hb + HX rat model may also be useful to study mechanisms of right heart failure in class 5 PH patients. Regardless, determining what extent extracellular Hb toxicity effects cardiomyocyte health and function, independent of its pulmonary vascular effects during the PH disease process, will be important in future studies.

The accumulation of lung tissue non-heme iron and increased oxidative stress in our model, suggest that either iron chelation or antioxidant treatments may provide viable alternatives to Hp therapy in mitigating the pathobiology associated with chronic Hb exposure. Previous work by our group and others suggest that the antioxidants and iron chelators do attenuate Hb mediated toxicity [9, 26]; However, the effects of the cell permeable iron chelators such as dexrazoxane [26] and deferoxamine [36] as well as the nitroxide antioxidant Tempol [9] appear to be less effective at protecting tissue from Hb toxicity compared to Hp used in this study. This may be a result of: (1) Hb's affinity for iron and the absence increased non-transferrin bound iron (NTBI) following Hb exposure; and/or (2) Hp's ability to limit extravascular compartmentalization of Hb. In our current study, NTBI is not increased amongst groups at terminal blood collection (data not shown), therefore, within the intra-vascular space the iron binding efficiency of chelators is likely of limited utility in our model. Furthermore, transferrin saturations trend higher in hypoxia, but are not different between groups (data not shown). Iron saturation do not reach levels that would lead to NTBI in plasma (>80% saturation) [37] Unlike extravascular hemolysis, where NTBI levels are found to be high and free plasma Hb is not detectible, these data suggest that in the presence of intra-vascular Hb exposure, binding and compartmentalizing Hb within the vascular space may be more effective strategy.

Study Limitations

Our Hb plus hypoxia PH model utilized for the present proof-of-principle study to determine efficacy for repeat dose Hp therapy was developed and characterized for broad-based application to diseases associated with Hb-induced pathology. Thus, it should be noted that our model cannot fully mimic a complicated disease process, such as SCD, but as previously mentioned shares phenotypic similarities with SCD by condensing Hb and hypoxia exposure experienced during the course of the disease process. This is considered within a time frame to allow for meaningful inferences to be made. However, there are some notable differences between how Hb and hypoxia are applied in our model compared to SCD. First, our model emulates the constant basal plasma concentrations of free Hb that are observed SCD patients due to low grade hemolysis, on to which we superimpose the effects of hypoxia. In contrast

to our model, higher concentrations of Hb occur with tissue hypoxia in an episodic manner associated with crisis during the SCD process. Because of the constant fluctuations in Hb concentration and degree of tissue hypoxia, the pulmonary vascular disease we observe in our rodent model could be more or less aggressive compared to the actual SCD process in humans; nonetheless our model does provide a basis to test therapeutic approaches for attenuating Hb's contribution to the pathophysiology of disease when concomitant hypoxia occurs.

Conclusion

The data presented here in a model of Hb-induced pathology that condenses a life time of intermittent Hb and Hx suggest that chronic low/moderate level extracellular Hb exposure acts as a disease modifying compound in PH. Repeated administrations of Hp attenuate cumulative effects and therefore further demonstrate: (1) the disease modifying role of Hb in PH; and (2) suggest a therapeutic role for Hp in disease processes involving chronic Hb exposures. In the present study, extracellular Hb increases pulmonary vascular lipid peroxidation, inflammation, remodeling, and resistance, as well as increases right ventricular hypertrophy and non-heme iron accumulation in pulmonary and cardiac tissue. The increase in pulmonary vascular resistance leads to greater RV hypertrophy and a faster progression toward right heart failure. The present results validate Hp as a potential therapeutic to attenuate the progression of PH exacerbation by extracellular Hb exposure, and suggest that further evaluation to determine the utility in patients with PH and RV failure secondary to hemolysis may be of clinical value.

Acknowledgements

We thank Julie Harral for her expertise in surgical pump implantation, acute and chronic rat catheterizations, and instrumentation to obtain pulmonary and systemic blood pressures and cardiac outputs.

Sources of funding:

This study was supported in part by the Giles F. Filley award from the American Physiological Society (Irwin DC) and National Heart, Lung and Blood Institute Grant 5P01HL014985-38(Stenmark KR).

The findings and conclusions in this article have not been formally disseminated by the Food and Drug Administration and should not be construed to represent any Agency determination or policy.

REFERENCES

1. Bunn HF, Nathan DG, Dover GJ, Hebbel RP, Platt OS, Rosse WF, Ware RE. Pulmonary hypertension and nitric oxide depletion in sickle cell disease. Blood. May 14; 2010 116(5):687–692. 2010. [PubMed: 20395414]
2. Hebbel RP. Reconstructing sickle cell disease: A data-based analysis of the “hyperhemolysis paradigm” for pulmonary hypertension from the perspective of evidence-based medicine. American Journal of Hematology. 2011; 86(2):123–154. [PubMed: 21264896]
3. Kato G, Taylor J. Pleiotropic effects of intravascular haemolysis on vascular homeostasis. British Journal of Hematology. 2009:1–12.
4. Simonneau G, Gatzoulis MA, Adatia I, Celermajer D, Denton C, Ghofrani A, Gomez Sanchez MA, Krishna Kumar R, Landzberg M, Machado RF, Olschewski H, Robbins IM, Souza R. Updated clinical classification of pulmonary hypertension. J Am Coll Cardiol. Dec 24; 2014 62(25 Suppl):D34–41. [PubMed: 24355639]

5. Dickinson MG, Bartelds B, Borgdorff MA, Berger RM. The role of disturbed blood flow in the development of pulmonary arterial hypertension: lessons from preclinical animal models. Am J Physiol Lung Cell Mol Physiol. Jul 1; 2013 305(1):L1–14. [PubMed: 23624788]
6. Shao D, Park JE, Wort SJ. The role of endothelin-1 in the pathogenesis of pulmonary arterial hypertension. Pharmacol Res. Jun; 2011 63(6):504–511. [PubMed: 21419223]
7. Tuder RM, Stacher E, Robinson J, Kumar R, Graham BB. Pathology of pulmonary hypertension. Clin Chest Med. Dec; 2013 34(4):639–650. [PubMed: 24267295]
8. Gladwin M, Vichinsky E. Pulmonary complications of sickle cell disease. New England journal of medicine. 2008; 359(21):2254–2265. [PubMed: 19020327]
9. Buehler PW, Baek JH, Lisk C, Connor I, Sullivan S, Kominsky D, Majka S, Stenmark KR, Nozik-Grayck E, Bonventura J, Irwin D. Free Hemolgobin Induction of Pulmonary Vascular Disease: Evidence for and inflammatory Mechanism. Am J Physiol Lung Cell Mol Physiol. Aug; 2012 303(4):312–326.
10. Schaer DJ, Buehler PW. Cell-free hemoglobin and its scavenger proteins: new disease models leading the way to targeted therapies. Cold Spring Harb Perspect Med. Jun.2013 3(6)
11. Belcher JD, Chen C, Nguyen J, Milbauer L, Abdulla F, Alayash AI, Smith A, Nath KA, Hebbel RP, Vercellotti GM. Heme triggers TLR4 signaling leading to endothelial cell activation and vaso-occlusion in murine sickle cell disease. Blood. Nov 25.2013
12. Lin S, Zhong Q, Lv F-L, Zhou Y, Li J-Q, Wang J-Z, Yang Q-W, Yin Q. Heme activates TLR4-mediated inflammatory injury via MyD88/TRIF signaling pathway in intracerebral hemorrhage. Journal of Neuroinflammation. 2012; 9(1):46. [PubMed: 22394415]
13. Piazza M, Damore G, Costa B, Gioannini T, Weiss J, Peri F. Hemin and a metabolic derivative coprohemin modulate TLR4 pathway differently through different molecular targets. Innate Immune. May 14; 2010 17(3):293–301.
14. Young KC, Hussein SM, Dadiz R, deMello D, Devia C, Hehre D, Suguihara C. Toll-like receptor 4-deficient mice are resistant to chronic hypoxia-induced pulmonary hypertension. Exp Lung Res. Mar; 2010 36(2):111–119. [PubMed: 20205596]
15. Nosslin BF, Nyman M. Haptoglobin determination in diagnosis of haemolytic diseases. Lancet. May 10; 1958 1(7028):1000–1001. [PubMed: 13540241]
16. Smithies O, Connell GE, Dixon GH. Inheritance of haptoglobin subtypes. Am J Hum Genet. Mar. 1962 14:14–21. [PubMed: 13914473]
17. Andersen CB, Torvund-Jensen M, Nielsen MJ, de Oliveira CL, Hersleth HP, Andersen NH, Pedersen JS, Andersen GR, Moestrup SK. Structure of the haptoglobin-haemoglobin complex. Nature. Sep 20; 2012 489(7416):456–459. [PubMed: 22922649]
18. Connell GE, Dixon GH, Smithies O. Subdivision of the three common haptoglobin types based on ‘hidden’ diffrences. Nature. Feb 3.1962 193:505–506. [PubMed: 13880879]
19. Boretti FS, Buehler PW, D'ÄôAgnillo F, Kluge K, Glaus T, Butt OI, Jia Y, Goede J, Pereira CP, Maggiorini M, Schoedon G, Alayash AI, Schaer DJ. Sequestration of extracellular hemoglobin within a haptoglobin complex decreases its hypertensive and oxidative effects in dogs and guinea pigs. The Journal of Clinical Investigation. 2009; 119(8):2271–2280. [PubMed: 19620788]
20. Hashimoto K, Nomura K, Nakano M, Sasaki T, Kurosawa H. Pharmacological intervention for renal protection during cardiopulmonary bypass. Heart Vessels. 1993; 8(4):203–210. [PubMed: 8307900]
21. Rother RP, Bell L, Hillmen P, Gladwin MT. The clinical sequelae of intravascular hemolysis and extracellular plasma hemoglobin: a novel mechanism of human disease. Jama. Apr 6; 2005 293(13):1653–1662. [PubMed: 15811985]
22. Frid MG, Brunetti JA, Burke DL, Carpenter TC, Davie NJ, Reeves JT, Roedersheimer MT, van Rooijen N, Stenmark KR. Hypoxia-induced pulmonary vascular remodeling requires recruitment of circulating mesenchymal precursors of a monocyte/macrophage lineage. Am J Pathol. Feb; 2006 168(2):659–669. [PubMed: 16436679]
23. Wiedermann BL, Olson JS. Acceleration of tetramer formation by the binding of inositol hexaphosphate to hemoglobin dimers. J Biol Chem. Jul 10; 1975 250(13):5273–5275. [PubMed: 238984]

24. Antonini, E.; Brunori, M. Hemoglobin and Myoglobin in their reactions with ligands. Vol. 21. North-Holland; Amersterdam: 1971.
25. Aebi H. Catalase in vitro. Methods Enzymol. 1984; 105:121–126. [PubMed: 6727660]
26. Butt OI, Buehler PW, D'Agnillo F. Blood-brain barrier disruption and oxidative stress in guinea pig after systemic exposure to modified cell-free hemoglobin. Am J Pathol. Mar; 2011 178(3): 1316–1328. [PubMed: 21356382]
27. Stenmark KR, Yeager ME, El Kasmi KC, Nozik-Grayck E, Gerasimovskaya EV, Li M, Riddle SR, Frid MG. The adventitia: essential regulator of vascular wall structure and function. Annu Rev Physiol. 2013; 75:23–47. [PubMed: 23216413]
28. Fagan KA, McMurtry I, Rodman DM. Nitric oxide synthase in pulmonary hypertension: lessons from knockout mice. Physiological research / Academia Scientiarum Bohemoslovaca. 2000; 49(5): 539–548. [PubMed: 11191358]
29. Buehler P, D'Agnillo F. Toxicological consequences of extracellular hemoglobin: Biochemical and physiological perspecrtives. Antioxidants & redox signaling. 2010; 12(2):275–291. [PubMed: 19659434]
30. Schaer DJ, Alayash AI. Clearance and Control Mechanisms of Hemoglobin from Cradle to Grave. Antioxidants & redox signaling. 2010; 12(2):181–184. [PubMed: 19788393]
31. Hod EA, Zhang N, Sokol SA, Wojczyk BS, Francis RO, Ansaldi D, Francis KP, Della-Latta P, Whittier S, Sheth S, Hendrickson JE, Zimring JC, Brittenham GM, Spitalnik SL. Transfusion of red blood cells after prolonged storage produces harmful effects that are mediated by iron and inflammation. Blood. May 27; 2010 115(21):4284–4292. [PubMed: 20299509]
32. Frid MG, Li M, Gnanasekharan M, Burke DL, Fragoso M, Strassheim D, Sylman JL, Stenmark KR. Sustained hypoxia leads to the emergence of cells with enhanced growth, migratory, and promitogenic potentials within the distal pulmonary artery wall. American Journal of Physiology - Lung Cellular and Molecular Physiology. Dec 1; 2009 297(6):L1059–L1072. 2009. [PubMed: 19767409]
33. El Kasmi KC, Pugliese SC, Riddle SR, Poth JM, Anderson AL, Frid MG, Li M, Pullamsetti SS, Savai R, Nagel MA, Fini MA, Graham BB, Tuder RM, Friedman JE, Eltzschig HK, Sokol RJ, Stenmark KR. Adventitial fibroblasts induce a distinct proinflammatory/profibrotic macrophage phenotype in pulmonary hypertension. J Immunol. Jul 15; 2014 193(2):597–609. [PubMed: 24928992]
34. Finn AV, Nakano M, Polavarapu R, Karmali V, Saeed O, Zhao X, Yazdani S, Otsuka F, Davis T, Habib A, Narula J, Kolodgie FD, Virmani R. Hemoglobin directs macrophage differentiation and prevents foam cell formation in human atherosclerotic plaques. J Am Coll Cardiol. Jan 10; 2012 59(2):166–177. [PubMed: 22154776]
35. Kremastinos DT, Farmakis D, Aessopos A, Hahalis G, Hamodraka E, Tsiapras D, Keren A. Beta-thalassemia cardiomyopathy: history, present considerations, and future perspectives. Circ Heart Fail. May; 2010 3(3):451–458. [PubMed: 20484195]
36. Cabrales P, Tsai AG, Intaglietta M. Deferoxamine lowers tissue damage after 80% exchange transfusion with polymerized hemoglobin. Antioxidants & redox signaling. Mar; 2007 9(3):375–384. [PubMed: 17184174]
37. Hershko C, Graham G, Bates GW, Rachmilewitz EA. Non-specific serum iron in thalassaemia: an abnormal serum iron fraction of potential toxicity. British journal of haematology. Oct; 1978 40(2):255–263. [PubMed: 708645]

HIGHLIGHTS

- Hb mediated lung injury is partially due to oxidative stress, lipid peroxidation and inflammation.
- Hb mediated pulmonary vascular remodeling occurs by an outside to inside phenomenon initiated in and around the lung blood vessel adventicia.
- Hp effectively binds free Hb in the vasculature and limits Hb access to tissue sites.
- Hp prevents Hb-induced tissue non-heme iron accumulation and oxidative stress in pulmonary and myocardial tissue.
- Hp normalizes functional indices of pulmonary hypertension.
- Hp administration may represent a therapeutic approach to mitigating chronic exposure to free Hb in certain disease states.

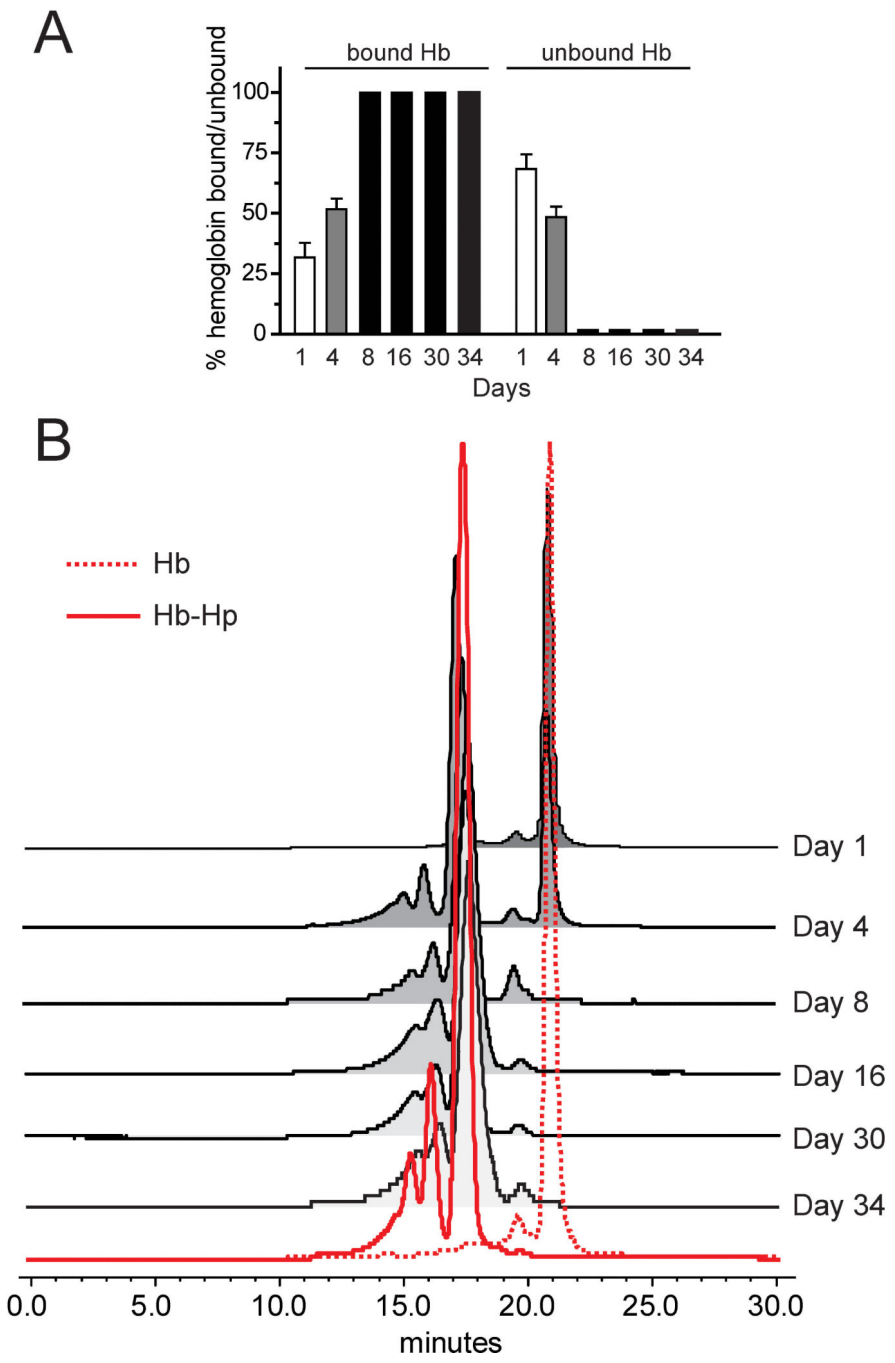

Figure 1. Infusion pump, plasma analysis of Hb-Hp complex

(A) Percentages of free and Hp bound Hb over 34 days of Hb infusion. (B) Chromatography of plasma from representative Hb exposed and Hp administered animals demonstrated a free Hb peak at an elution time of 21 minutes. This was confirmed by the chromatographic profile of Hb standard solution shown as a dotted red trace. An elution time shift to a broad band of peaks eluting over 13-17.5 minutes was observed as extra-cellular plasma Hb became bound to Hp. Hb- hemoglobin, Hp-haptoglobin.

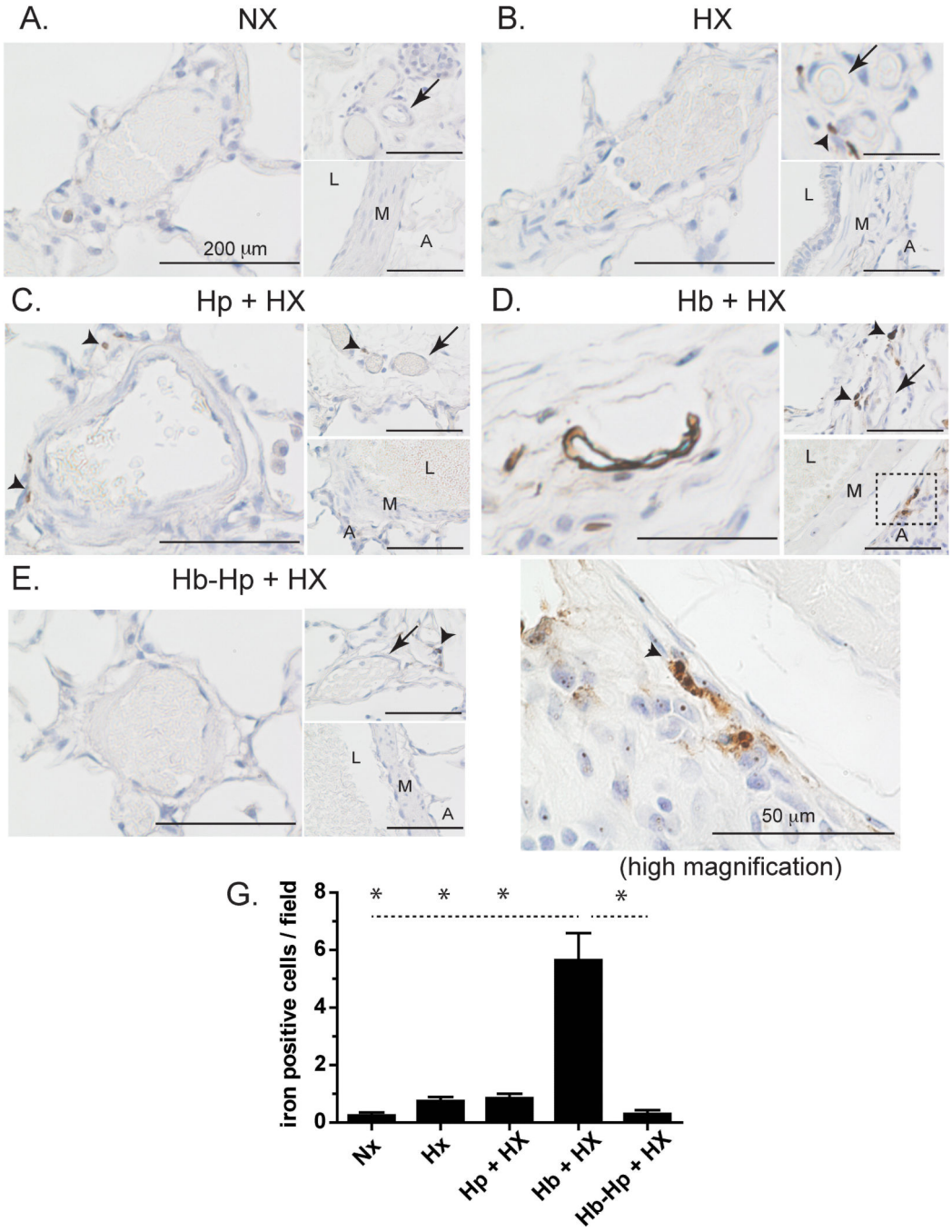

Figure 2. Lung iron accumulation

Localization of non-heme iron in the lungs of either normoxic control animals or animals exposed to free Hb infusion plus hypoxia in the presence of absence of Hp. * p <0.001 Hb +HX vs. all other groups L- Lumen. M- Media. A-adventicia. NX- normoxia. HX-hypoxia, Hb- hemoglobin, Hp- haptoglobin. Black arrows- regions of iron accumulation.

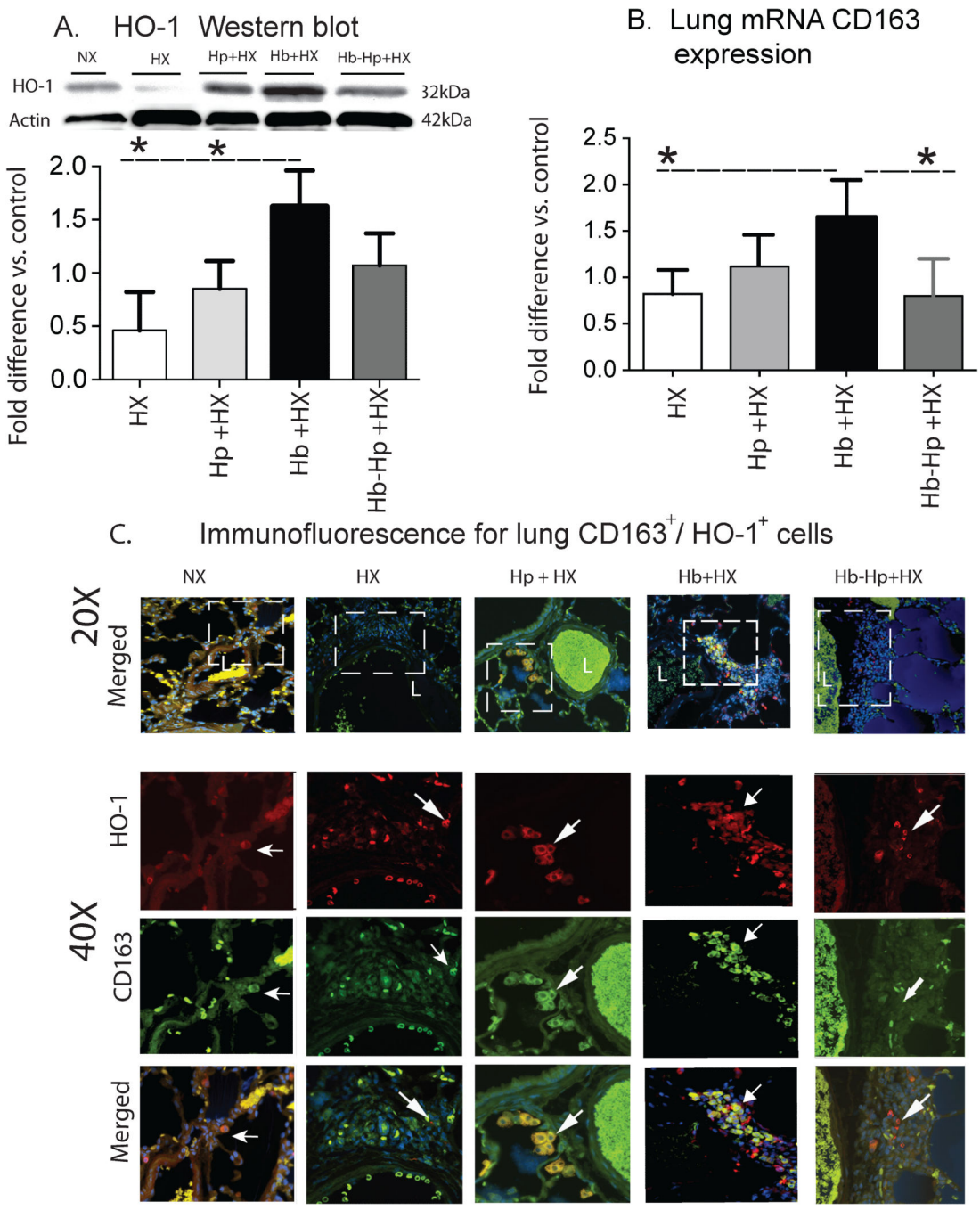

Figure 3. Quantification and localization of HO-1 lung expressionan

(A) Western Blot analyses of lung HO-1 from densitometry analysis. **(B)** qRT-PCR analysis of whole lung CD163 mRNA . **(C)** Representative microphotographs of stained lung sections for HO-1 localization. 40X are high magnification of white boxed areas.HO-1 expression- (red), CD163 (green) and DAPI-. L- vessel lumen. White arrows show areas of HO-1 and CD163 co-expression. * p< 0.04 Hb+HX vs. all other groups. NX- normoxia. HX-hypoxia. Hb- hemoglobin. Hp- haptoglobin.

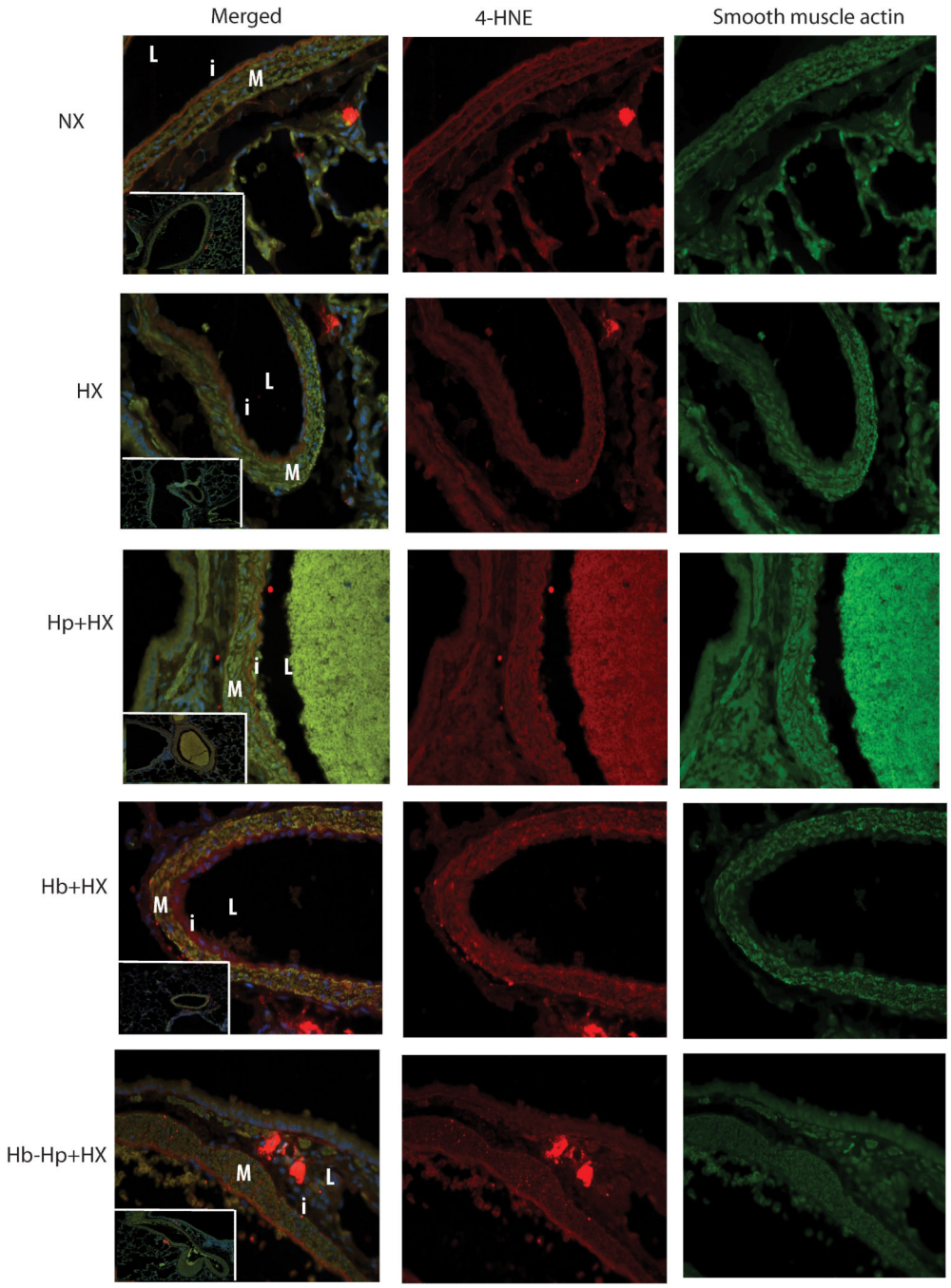

Figure 4. Lung vascular 4-hydroxynonenal (4-HNE)

Microphotographs of stained lung sections of 4-hydroxynonenal localization. Pictures captured at 40X are high magnification of the vessels in the white box captured at 10x. M-media. L-lumen. i- Intima. SMA- smooth muscle actin. 4-HNE- 4-hydroxynonenal. NX-Normoxia. HX-Hypoxia. Hp- Haptoglobin. Hb-Hemoglobin

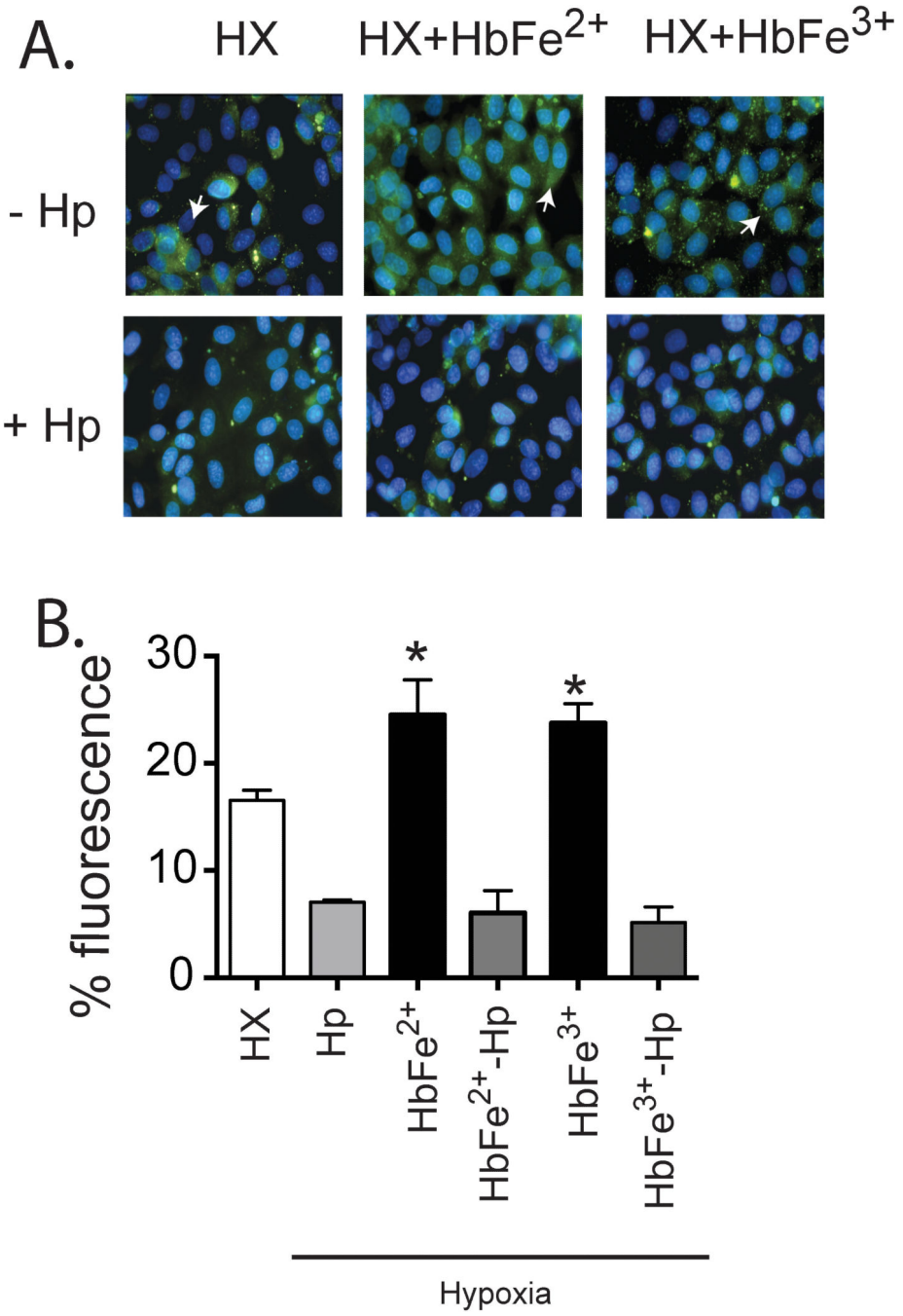

Figure 5. Hb induced lipid peroxidation in rat pulmonary artery endothelial cells exposed to hypoxia

(A) photomicrographs that show areas of lipid perioxidation. (B) Image J quantification of lipid peroxidation. Green lipid peroxidation- (White arrows). HX-Hypoxia. Hb-Hemoglobin.Hp-Haptoglobin. * $p<0.05$ vs. all other groups.

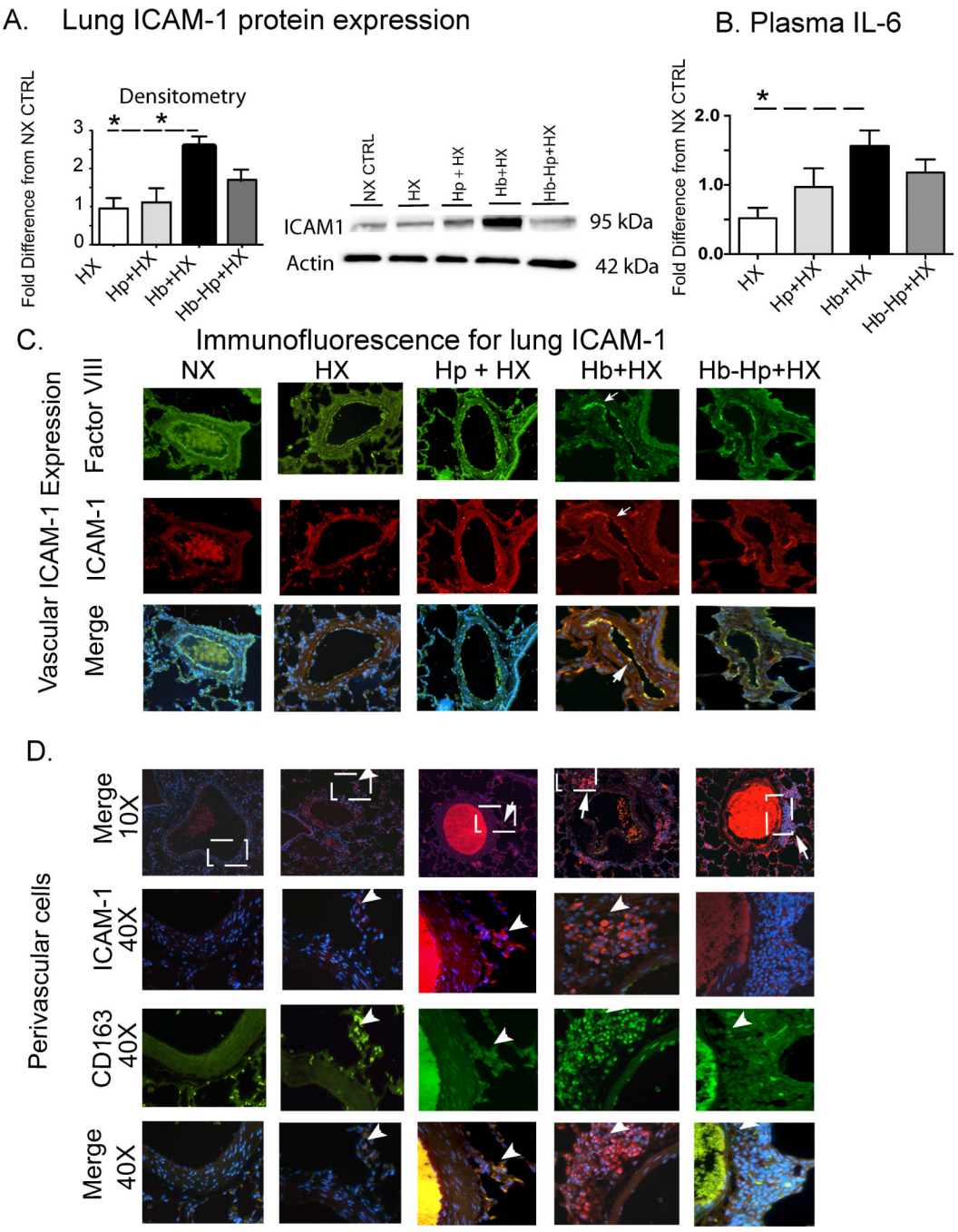

Figure 6. Quantification and localization of ICAM-1 lung expressionan and plasma IL-6 concentration

(A) Whole lung ICAM-1 protein expression. **(B)** Plasma IL-6 concentration. **(C and D)** Representative microphotographs of stained lung sections showing ICAM expression in the endothelium and extravascular cells respectively. White boxes show the regions that 40X microphotographs were captured. ICAM expression- (red), Factor VIII (green) and DAPI.White arrows show regions of ICAM expression. * p< 0.04 Hb+HX vs. HX and Hp +HX groups. NX- normoxia. HX- hypoxia. Hb- hemoglobin. Hp- haptoglobin.

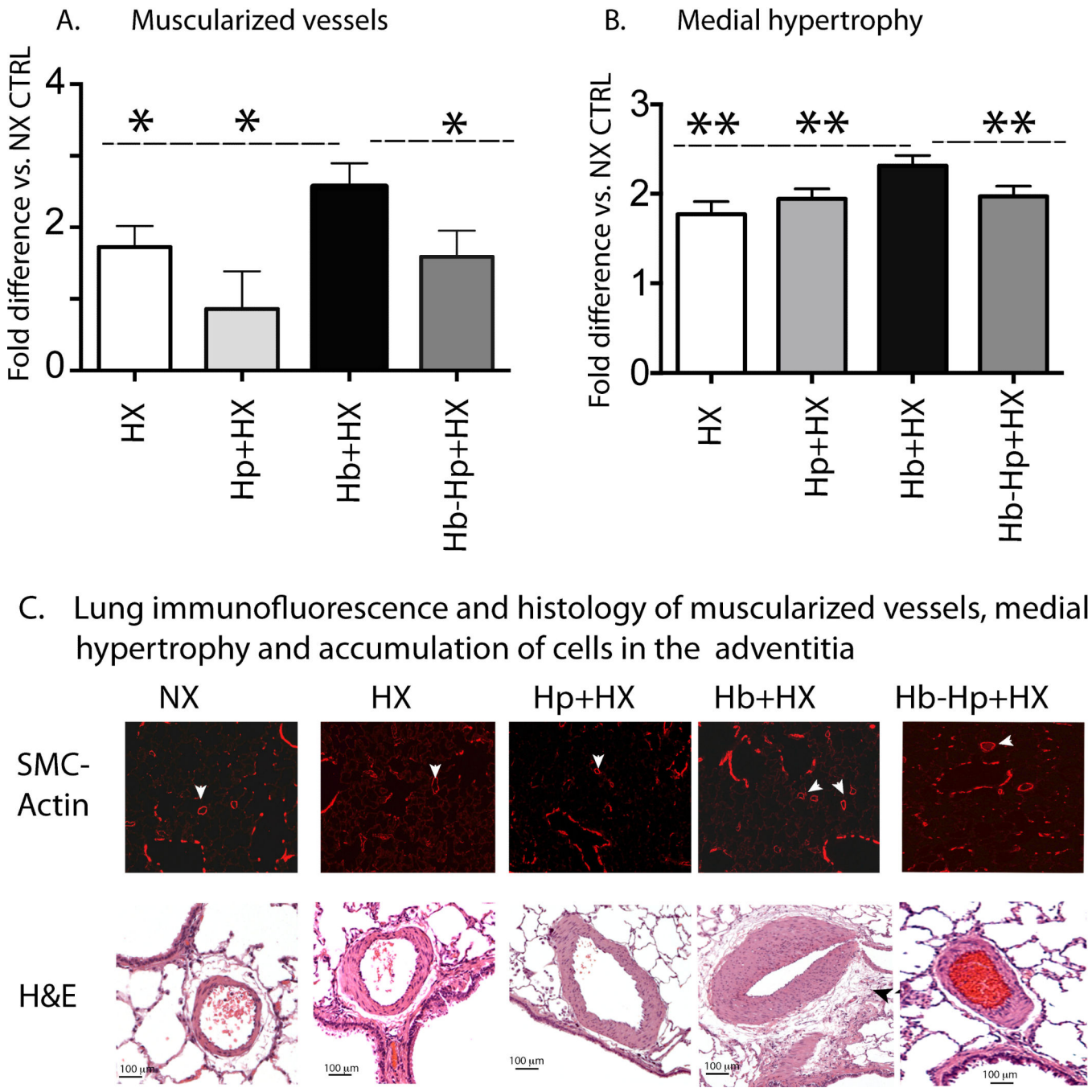

Figure 7. Hb mediated pulmonary vascular remodeling is attenuated with Hp therapy

(A) Quantification of muscularization of small arteries. **(B)** Quantification of medial hypertrophy of pulmonary arteries**. (C)** Microphotographs of lungs stained with -smooth muscle actin or hematoxylin and eosin (H&E) to visualize small arterial muscularization, medial hypertrophy and accumulation of cells in the adventitia compartment. White arrows show muscularized small arteries, black arrows show the accumulation of cells in the advanticia surrounding the vessel. * $p < 0.044$ Hb+HX vs. all other groups (one tailed test).

** $p < 0.04$ Hb+HX vs. all other groups. NX- normoxia. HX-hypoxia. Hb- hemoglobin. Hp-haptoglobin.

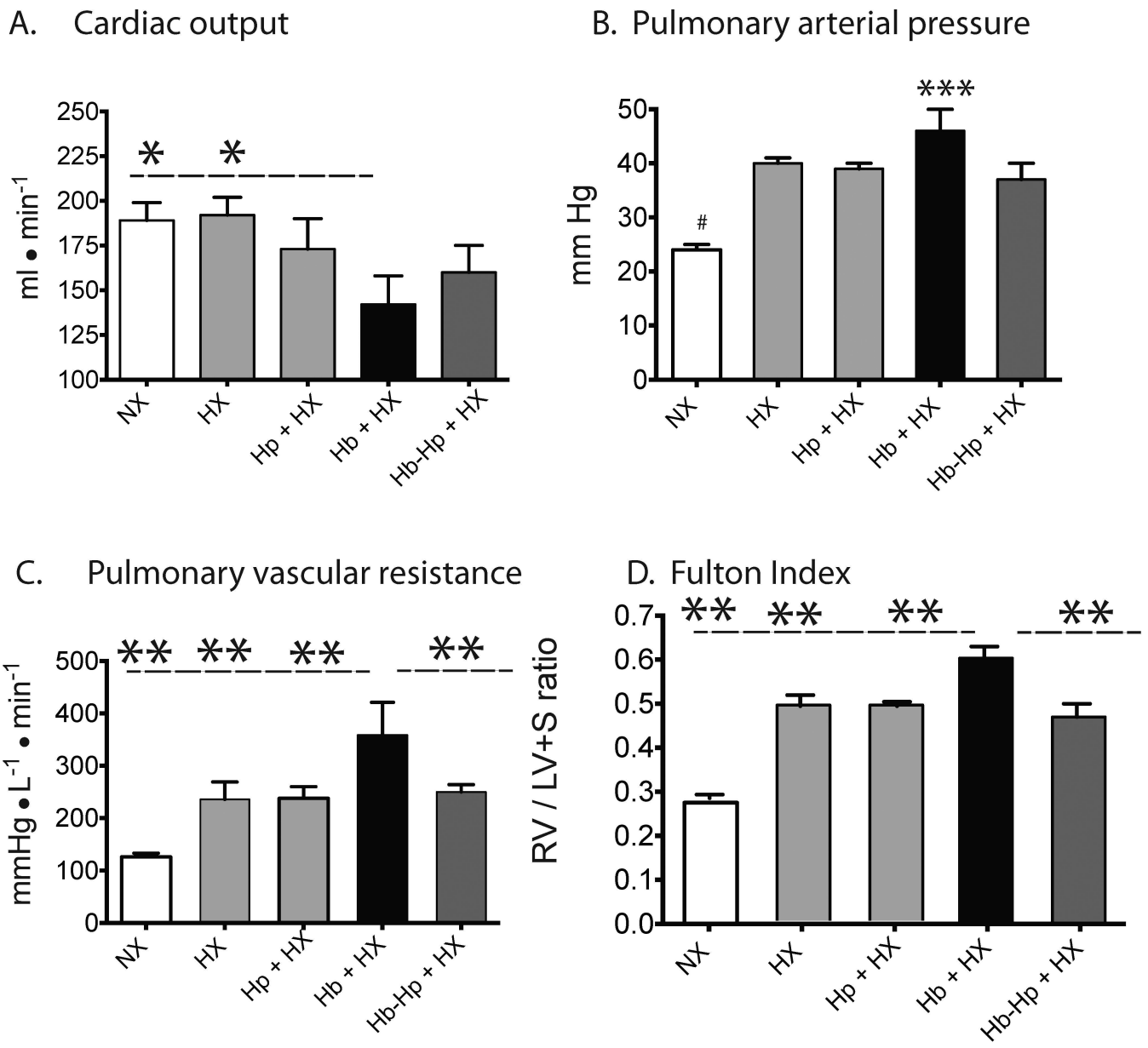

Figure 8. Hemodynamic characterization of pulmonary arterial hypertension

(A) Cardiac output. (B) Pulmonary arterial pressures. (C) Pulmonary vascular resistance. (E) Fulton index of right ventricular hypertrophy. * $p < 0.03$ Hb+HX vs. NX and HX; ** $p < 0.0.048$ Hb+HX vs. all other cohorts; # $p<0.001$ NX vs. all other cohorts; *** $p=0.2$ Hb +HX vs. HX. NX- normoxia. HX-hypoxia. Hb- hemoglobin. Hp- haptoglobin

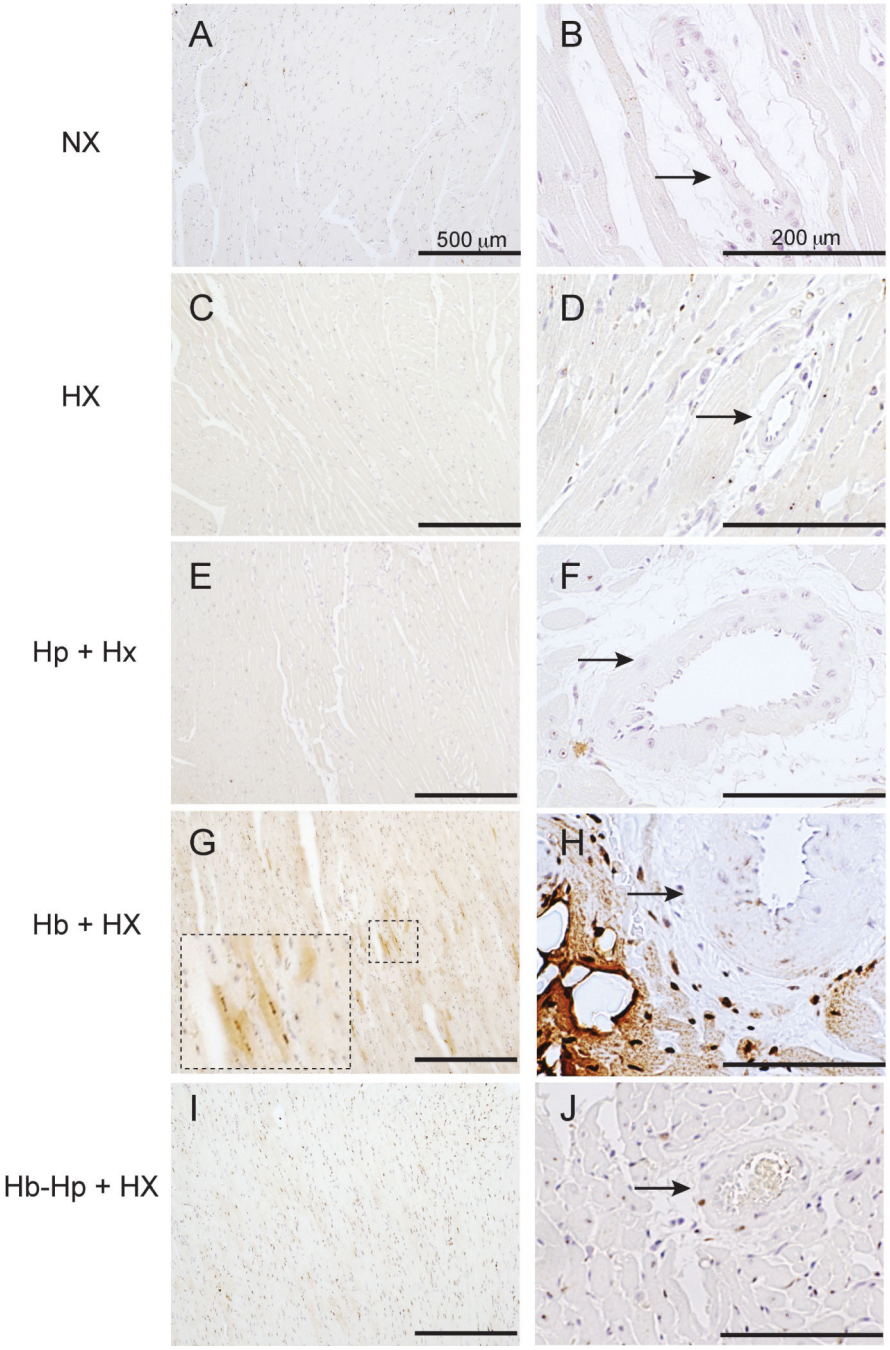

Figure 9. Heart iron accumulation

Localization of non-heme iron in the cardiac tissue of either NX control animals or animals exposed to free Hb infusion plus HX in the presence of absence of Hp. HX-hypoxia, Hb-hemolglobin, Hp- haptoglobin.